INTERNATIONAL JOURNAL FOR NUMERICAL METHODS IN ENGINEERING
Int. J. Numer. Meth. Engng 2009; **78**:32–47
Published online 20 October 2008 in Wiley InterScience (www.interscience.wiley.com). DOI: 10.1002/nme.2472

Explicit expressions for 3D boundary integrals in potential theory‡

S. Nintcheu Fata*, †

Computer Science and Mathematics Division, Oak Ridge National Laboratory, P.O. Box 2008, MS 6367, Oak Ridge, TN 37831-6367, U.S.A.

SUMMARY

On employing isoparametric, piecewise linear shape functions over a flat triangular domain, exact expressions are derived for all surface potentials involved in the numerical solution of three-dimensional singular and hyper-singular boundary integral equations of potential theory. These formulae, which are valid for an arbitrary source point in space, are represented as analytic expressions over the edges of the integration triangle. They can be used to solve integral equations defined on polygonal boundaries via the collocation method or may be utilized as analytic expressions for the inner integrals in the Galerkin technique. In addition, the constant element approximation can be directly obtained with no extra effort. Sample problems solved by the collocation boundary element method for the Laplace equation are included to validate the proposed formulae. Copyright © 2008 John Wiley & Sons, Ltd.

Received 15 May 2008; Revised 11 July 2008; Accepted 21 August 2008

KEY WORDS: analytic integration; singular integrals; boundary integral method; triangular boundary; potential theory

1. INTRODUCTION

The numerical treatment of 3D potential problems by the boundary element method (BEM) often requires the computation of nearly, weakly, strongly, and hyper-singular surface integrals. Accurate and efficient evaluations of these potentials at an arbitrary point on and near the polygonal surface of a 3D polyhedral domain represent a major task in the boundary integral equation (BIE) method [1–4]. In practice, the faces of the polyhedron are usually formed with triangles and constant or linear interpolations are often employed to approximate the potential and flux on each triangle.

*Correspondence to: S. Nintcheu Fata, Computer Science and Mathematics Division, Oak Ridge National Laboratory, P.O. Box 2008, MS 6367, Oak Ridge, TN 37831-6367, U.S.A.
†E-mail: nintcheufats@ornl.gov

Contract/grant sponsor: The U.S. Government; contract/grant number: DE-AC05-00OR22725

Over the past decades, several numerical approximations [5–8] have been proposed for the evaluation of singular and hyper-singular integrals. For the treatment of nearly singular integrals, which occur when the source point is 'close to', but not on, the integration polygon, various computational methodologies are available [9–12]. Moreover, analytic integration techniques [13–17] have also been developed to deal with integrals over triangular boundaries using piecewise linear approximations. Expressed in a coordinate system, local with respect to the integration triangle, these analytic methods provide exact formulae to calculate various potentials defined over a triangle as a whole. Although very effective for collocation BEM, using existing analytic formulae to evaluate the inner integral in the hyper-singular Galerkin BEM is still tedious and fraught with difficulties.

To alleviate these impediments, a new set of exact expressions representing various potentials defined over a flat triangle are proposed. These formulae, which are valid for an arbitrary source point, are derived for all potentials frequently found in the numerical treatment of 3D singular and hyper-singular BIEs with linear shape functions. They are given as analytic formulae over the sides (edges) of the integration triangle. Indeed, the proposed formulae have the same format for each side of the integration triangle. Compared with existing analytic representations, this recursive format is very advantageous as it renders subsequent singularity analysis by the Galerkin method manageable.

Details of the derivation as well as examples to validate the proposed formulae are included.

2. PROBLEM FORMULATION

Consider the numerical treatment of the Laplace equation

$$\nabla^2 u = 0 \tag{1}$$

in a bounded domain $\Omega \subset \mathbb{R}^3$ with boundary Γ via a BIE method. Upon specifying by $\mathbf{n}$ the unit normal to Γ directed toward the exterior of Ω, let $t = \partial u/\partial n$ be the flux associated with the potential u. Also, let $\mathbf{x}_\varepsilon$ be an exterior point to $\overline{\Omega} = \Omega \cup \Gamma$, i.e. $\mathbf{x}_\varepsilon \in \mathbb{R}^3 \setminus \overline{\Omega}$.

On employing the Green's representation formula [2, 18, 19], the potential u and flux t on Γ can be obtained by solving the singular BIE

$$\lim_{\mathbf{x}_\varepsilon \to \mathbf{x} \in \Gamma} \left(\int_\Gamma G(\mathbf{x}_\varepsilon, \mathbf{y}) t(\mathbf{y}) \, \mathrm{d}\Gamma_\mathbf{y} - \int_\Gamma \mathbf{H}(\mathbf{x}_\varepsilon, \mathbf{y}) \cdot \mathbf{n}(\mathbf{y}) u(\mathbf{y}) \, \mathrm{d}\Gamma_\mathbf{y} \right) = 0 \tag{2}$$

where the weakly singular and strongly singular kernels, G and $\mathbf{H}$, are given respectively, by

$$G(\mathbf{x}, \mathbf{y}) = \frac{1}{4\pi} \frac{1}{\|\mathbf{x} - \mathbf{y}\|}, \quad \mathbf{H}(\mathbf{x}, \mathbf{y}) = \frac{1}{4\pi} \frac{\mathbf{x} - \mathbf{y}}{\|\mathbf{x} - \mathbf{y}\|^3}, \quad \mathbf{x}, \mathbf{y} \in \mathbb{R}^3, \ \ \mathbf{x} \neq \mathbf{y} \tag{3}$$

In (3), $\mathbf{x}$ is usually called the source point and $\mathbf{y}$ is termed the receiver or field point.

2.1. Numerical approximation

With reference to Figure 1, assume that Γ is the surface of a polyhedron. With this assumption, consider a triangulation of $\Gamma = \bigcup \overline{E_q}$ into closed and non-overlapping surface elements such that

DOI: 10.1002/nme

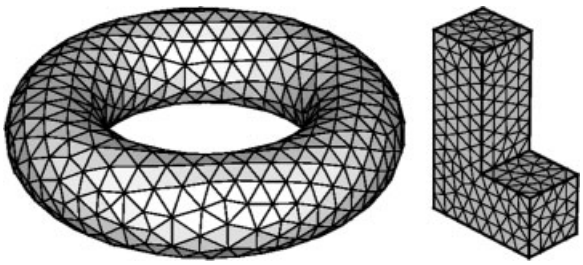

Figure 1. Left: triangulation of a torus featuring 1076 triangles with 538 nodes. Right: discretization of an L-shaped domain with 578 triangles and 401 nodes.

E_q is an open flat triangle. Let N_E be the total number of elements (triangles) on Γ. A standard procedure in the numerical treatment of (2) is to decompose the boundary potential u and flux t in terms of respective nodal values and basis shape functions ψ_j at discrete points $\mathbf{y}^j$ on Γ as

$$u(\mathbf{y}) = \sum_{j=1}^{N} u(\mathbf{y}^j)\psi_j(\mathbf{y}), \quad t(\mathbf{y}) = \sum_{j=1}^{N} t(\mathbf{y}^j)\psi_j(\mathbf{y}), \quad \mathbf{y}^j, \mathbf{y} \in \Gamma \tag{4}$$

where N is the total number of boundary nodes on Γ. In this study, ψ_j will be specified as piecewise linear shape functions.

With these definitions, a collocation method for resolving (2) requires that the singular BIE is satisfied exactly at a set of collocation points $\{\mathbf{x}^i\}_{i=1}^{N}$ resting on Γ. This requirement leads to a dense linear system of algebraic equations for boundary potential u and flux t

$$\mathbf{G}\{t\} = \mathbf{H}\{u\} \tag{5}$$

where $\{u\}$ and $\{t\}$ are vectors containing nodal potentials $u(\mathbf{y}^j)$ and fluxes $t(\mathbf{y}^j)$, respectively; components of influence matrices $\mathbf{G}$ and $\mathbf{H}$ take the form

$$\begin{aligned} G_{ij} &= \sum_{q=1}^{N_{E_j}} \lim_{\mathbf{x}_\varepsilon \to \mathbf{x}^i} \int_{E_q} G(\mathbf{x}_\varepsilon, \mathbf{y})\psi_j(\mathbf{y})\, \mathrm{d}\Gamma_{\mathbf{y}} \\ H_{ij} &= \sum_{q=1}^{N_{E_j}} \lim_{\mathbf{x}_\varepsilon \to \mathbf{x}^i} \int_{E_q} \mathbf{H}(\mathbf{x}_\varepsilon, \mathbf{y})\cdot\mathbf{n}(\mathbf{y})\psi_j(\mathbf{y})\, \mathrm{d}\Gamma_{\mathbf{y}}, \quad \mathbf{x}^i \in \Gamma \end{aligned} \tag{6}$$

where the triangle $E_q \in \mathrm{supp}(\psi_j)$ and N_{E_j} is the number of boundary elements in $\mathrm{supp}(\psi_j)$.

Upon prescribing the boundary conditions for the specific boundary-value problem associated with (1), the linear system (5) can be rearranged as

$$\mathbf{A}\{z\} = \{b\} \tag{7}$$

where all unknown quantities on the boundary Γ have been collected in $\{z\}$, and $\{b\}$ is a vector whose entries are obtained from known boundary data.

DOI: 10.1002/nme

2.2. Surface potentials over a triangle

In view of the influence coefficients (6), let the source point $\mathbf{x}\in\mathbb{R}^3$. Now, define the single-layer potential

$$G_j^q(\mathbf{x})=\int_{E_q} G(\mathbf{x},\mathbf{y})\psi_j(\mathbf{y})\,\mathrm{d}\Gamma_{\mathbf{y}} \tag{8}$$

and the double-layer potential

$$H_j^q(\mathbf{x})=\int_{E_q} \mathbf{H}(\mathbf{x},\mathbf{y})\cdot\mathbf{n}(\mathbf{y})\psi_j(\mathbf{y})\,\mathrm{d}\Gamma_{\mathbf{y}} \tag{9}$$

over a generic triangle E_q. In addition to (8) and (9), consider the double-layer potential

$$\mathbf{S}_j^q(\mathbf{x})=-\int_{E_q} \mathbf{H}(\mathbf{x},\mathbf{y})\psi_j(\mathbf{y})\,\mathrm{d}\Gamma_{\mathbf{y}} \tag{10}$$

and 'quadruple-layer' potential

$$\mathbf{T}_j^q(\mathbf{x})=\int_{E_q} \mathbf{T}(\mathbf{x},\mathbf{y})\cdot\mathbf{n}(\mathbf{y})\psi_j(\mathbf{y})\,\mathrm{d}\Gamma_{\mathbf{y}} \tag{11}$$

over E_q, where the hyper-singular kernel

$$\mathbf{T}(\mathbf{x},\mathbf{y})=\frac{1}{4\pi}\left[\frac{\mathbf{I}_2}{\|\mathbf{x}-\mathbf{y}\|^3}-3\frac{(\mathbf{x}-\mathbf{y})\otimes(\mathbf{x}-\mathbf{y})}{\|\mathbf{x}-\mathbf{y}\|^5}\right],\quad \mathbf{x},\mathbf{y}\in\mathbb{R}^3,\ \ \mathbf{x}\neq\mathbf{y} \tag{12}$$

with $\mathbf{I}_2$ representing the symmetric, second-order identity tensor on $\mathbb{R}^3$. Potentials (10) and (11) appear in the treatment of the Laplace equation via hyper-singular Galerkin BIE over triangular surfaces as part of the inner integrals of the influence coefficients. Given the fundamental importance of computing surface potentials (8) through (11) in the boundary integral analysis of potential problems, the aim of this study is to provide explicit formulae for evaluating these potentials when ψ_j is a *linear* shape function over a flat triangle E_q.

3. EXACT EVALUATION ON SURFACE POTENTIALS OVER A TRIANGLE

With reference to a Cartesian frame $\{\mathbf{0};x_1,x_2,x_3\}$, let $\{\mathbf{y}^1,\mathbf{y}^2,\mathbf{y}^3\}\subset\mathbb{R}^3$ be the position vectors of the vertices of the generic triangle E_q (see Figure 2). Also, let $L_q=\partial E_q$ and define the oriented segments of L_q as $L_1=[\mathbf{y}^1,\mathbf{y}^2]$, $L_2=[\mathbf{y}^2,\mathbf{y}^3]$, $L_3=[\mathbf{y}^3,\mathbf{y}^1]$. Now, let $\{\mathbf{x};\mathbf{e}_1,\mathbf{e}_2,\mathbf{e}_3\}$ be the local orthonormal companion reference of $\mathbb{R}^3$ such that (i) the unit vector $\mathbf{e}_1$ is parallel to L_1, and (ii) $\mathbf{e}_3\perp E_q$ and points in the direction of the unit 'outward' normal to Γ on E_q. Note that the basis vector $\mathbf{e}_i$ is constant on E_q. Further, denote by P_{E_q} the plane of E_q spanned by $\{\mathbf{e}_1,\mathbf{e}_2\}$ and let $\underset{\sim}{\mathbf{x}}\in P_{E_q}$ be the orthogonal projection of the source point $\mathbf{x}$ on P_{E_q} in the direction $\mathbf{e}_3$. In what follows, $\{\underset{\sim}{\mathbf{x}};\mathbf{e}_1,\mathbf{e}_2\}$ is the induced reference on P_{E_q}.

These definitions introduce a local coordinate system $\{\mathbf{x};\xi,\zeta,\eta\}$ associated with E_q in $\mathbb{R}^3$. In $\{\mathbf{x};\mathbf{e}_1,\mathbf{e}_2,\mathbf{e}_3\}$, the position vector $\mathbf{r}$ of an arbitrary field point $\mathbf{y}$ can be decomposed as

$$\mathbf{r}=\mathbf{y}-\mathbf{x}\equiv\mathbf{y}_{\mathbf{x}}=\xi\mathbf{e}_1+\zeta\mathbf{e}_2+\eta\mathbf{e}_3 \tag{13}$$

DOI: 10.1002/nme

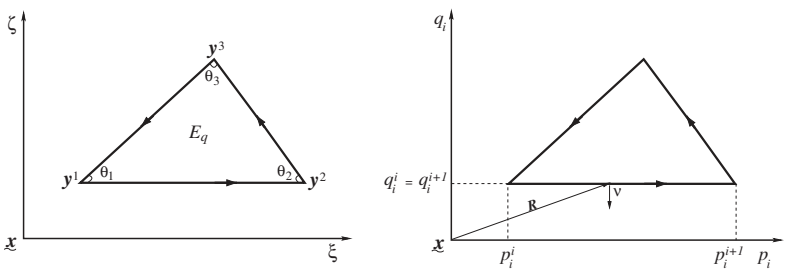

Figure 2. Local coordinate systems associated with a generic triangle E_q.

so that

$$r = \|\mathbf{y} - \mathbf{x}\| = \sqrt{\xi^2 + \zeta^2 + \eta^2} \tag{14}$$

In addition, the position vectors $\mathbf{r}^j$ of the respective vertices $\mathbf{y}^j$ of E_q can be written as

$$\mathbf{r}^j = \mathbf{y}^j - \mathbf{x} \equiv \mathbf{y}^j_{\mathbf{x}} = \xi_j \mathbf{e}_1 + \zeta_j \mathbf{e}_2 + \eta \mathbf{e}_3, \quad j = 1, 2, 3 \tag{15}$$

In this setting, the parameter η characterizes the relative distance (elevation) of the source point $\mathbf{x}$ to the $\xi\zeta$-plane (i.e. P_{E_q}). By construction, $\zeta_1 = \zeta_2$. Upon setting $\Delta = (\xi_2 - \xi_1)(\zeta_3 - \zeta_1)$, the linear shape functions ψ_j on E_q can be expressed as

$$\psi_j = a_j \xi + b_j \zeta + c_j, \quad j = 1, 2, 3 \tag{16}$$

where

$$\begin{aligned} a_1 &= -\frac{1}{\xi_2 - \xi_1}, \quad b_1 = \frac{\xi_3 - \xi_2}{\Delta}, \quad c_1 = \frac{\xi_2\zeta_3 - \xi_3\zeta_2}{\Delta} \\ a_2 &= \frac{1}{\xi_2 - \xi_1}, \quad b_2 = \frac{\xi_1 - \xi_3}{\Delta}, \quad c_2 = \frac{\xi_3\zeta_1 - \xi_1\zeta_3}{\Delta} \\ a_3 &= 0, \quad b_3 = \frac{1}{\zeta_3 - \zeta_1}, \quad c_3 = -\frac{\zeta_1}{\zeta_3 - \zeta_1} \end{aligned} \tag{17}$$

Note that c_j $(j = 1, 2, 3)$ depends on the source point $\mathbf{x}$, i.e. $c_j = c_j(\mathbf{x})$.

3.1. Generic integrals

To show that surface potentials (8) through (11) can be calculated exactly, it is important to first establish their decomposition into some generic integrals. To this end, one can use (3), (13), (14), (16) to verify that the single- and double-layer potentials (8) and (9) take the form

$$G^q_j(\mathbf{x}) = \frac{1}{4\pi}[a_j I^\xi_1 + b_j I^\zeta_1 + c_j I_1], \quad H^q_j(\mathbf{x}) = \frac{-\eta}{4\pi}[a_j I^\xi_3 + b_j I^\zeta_3 + c_j I_3] \tag{18}$$

DOI: 10.1002/nme

where the generic integrals are given by

$$\begin{aligned} I_1 &= \int_{E_q} \frac{1}{r}\,\mathrm{d}s, \quad I_1^{\xi} = \int_{E_q} \frac{\xi}{r}\,\mathrm{d}s, \quad I_1^{\zeta} = \int_{E_q} \frac{\zeta}{r}\,\mathrm{d}s \\ I_3 &= \int_{E_q} \frac{1}{r^3}\,\mathrm{d}s, \quad I_3^{\xi} = \int_{E_q} \frac{\xi}{r^3}\,\mathrm{d}s, \quad I_3^{\zeta} = \int_{E_q} \frac{\zeta}{r^3}\,\mathrm{d}s \end{aligned} \tag{19}$$

Similarly, the double- and 'quadruple'-layer potentials (10) and (11) can be evaluated effectively by means of $I_3, I_3^{\xi}, I_3^{\zeta}$ expressed in (19) and the additional generic integrals

$$\begin{aligned} I_3^{\xi\xi} &= \int_{E_q} \frac{\xi^2}{r^3}\,\mathrm{d}s, \quad I_3^{\xi\zeta} = \int_{E_q} \frac{\xi\zeta}{r^3}\,\mathrm{d}s, \quad I_3^{\zeta\zeta} = \int_{E_q} \frac{\zeta^2}{r^3}\,\mathrm{d}s \\ I_5 &= \int_{E_q} \frac{1}{r^5}\,\mathrm{d}s, \quad I_5^{\xi} = \int_{E_q} \frac{\xi}{r^5}\,\mathrm{d}s, \quad I_5^{\zeta} = \int_{E_q} \frac{\zeta}{r^5}\,\mathrm{d}s \\ I_5^{\xi\xi} &= \int_{E_q} \frac{\xi^2}{r^5}\,\mathrm{d}s, \quad I_5^{\xi\zeta} = \int_{E_q} \frac{\xi\zeta}{r^5}\,\mathrm{d}s, \quad I_5^{\zeta\zeta} = \int_{E_q} \frac{\zeta^2}{r^5}\,\mathrm{d}s \end{aligned} \tag{20}$$

3.2. Analytic formulae

To give exact expressions of the generic integrals (19) and (20) over L_q, let $\theta_i \in (0, \pi)$ be the inclusion angle at vertex $\mathbf{y}^i$ $(i = 1, 2, 3)$ of E_q so that $\theta_1 + \theta_2 + \theta_3 = \pi$ (see Figure 2). In addition, define

$$\alpha_1 \equiv 0, \quad \alpha_2 = \pi - \theta_2, \quad \alpha_3 = \pi + \theta_1 \tag{21}$$

With the aid of (21), one can introduce three local orthonormal companion references of $\mathbb{R}^3$ with origin at the source point $\mathbf{x}$, $\{\mathbf{x}; \mathbf{e}_{p_i}, \mathbf{e}_{q_i}, \mathbf{e}_3\}$, such that $\mathbf{e}_{p_i}$ is parallel to L_i $(i = 1, 2, 3)$ and $\mathbf{e}_3 \perp E_q$. Note that $\{\mathbf{x}; \mathbf{e}_{p_1}, \mathbf{e}_{q_1}, \mathbf{e}_3\} \equiv \{\mathbf{x}; \mathbf{e}_1, \mathbf{e}_2, \mathbf{e}_3\}$. References $\{\mathbf{x}; \mathbf{e}_{p_i}, \mathbf{e}_{q_i}, \mathbf{e}_3\}$ induce local coordinate systems $\{\mathbf{x}; p_i, q_i, \eta\}$ associated with each side (edge) L_i of E_q in $\mathbb{R}^3$ such that

$$\begin{aligned} p_i &= \xi \cos\alpha_i + \zeta \sin\alpha_i \\ q_i &= -\xi \sin\alpha_i + \zeta \cos\alpha_i \end{aligned} \tag{22}$$

As a result, $\{\underset{\sim}{\mathbf{x}}; p_i, q_i\}$, which are defined for every oriented side L_i of E_q, are local coordinate systems on P_{E_q}. Now, let (p_i^j, q_i^j, η) be the local coordinate in $\{\mathbf{x}; \mathbf{e}_{p_i}, \mathbf{e}_{q_i}, \mathbf{e}_3\}$ of the jth vertex $\mathbf{r}^j$ of E_q. In view of (15), the distance between the source point $\mathbf{x}$ and the vertex $\mathbf{y}^j$ can be written as

$$\rho_j = \sqrt{(p_i^j)^2 + (q_i^j)^2 + \eta^2} \tag{23}$$

By construction,

$$q_1^1 = q_1^2 \equiv q_1, \quad q_2^2 = q_2^3 \equiv q_2, \quad q_3^3 = q_3^1 \equiv q_3 \tag{24}$$

To aid the ensuing development, let

$$\tilde{\rho}_1(\mathbf{x}) = \rho_1 - \rho_2, \quad \tilde{\rho}_2(\mathbf{x}) = \rho_2 - \rho_3, \quad \tilde{\rho}_3(\mathbf{x}) = \rho_3 - \rho_1, \quad d_i = (q_i)^2 + \eta^2, \quad i = 1, 2, 3$$

DOI: 10.1002/nme

Further, define the following generic functions for each oriented side $L_i=[\mathbf{y}^i,\mathbf{y}^{i+1}]$ of E_q as

$$\begin{aligned}
&\gamma_i(\mathbf{x})=\arctan\left(\frac{-2p_i^iq_i\eta\rho_i}{(q_i)^2(\rho_i)^2-(p_i^i)^2\eta^2}\right)-\arctan\left(\frac{-2p_i^{i+1}q_i\eta\rho_{i+1}}{(q_i)^2(\rho_{i+1})^2-(p_i^{i+1})^2\eta^2}\right)\\
&\chi_i(\mathbf{x})=\ln[p_i^i+\rho_i]-\ln[p_i^{i+1}+\rho_{i+1}],\quad \delta_i(\mathbf{x})=\frac{p_i^i}{\rho_i}-\frac{p_i^{i+1}}{\rho_{i+1}},\quad \mathscr{L}_i(\mathbf{x})=\frac{1}{\rho_i}-\frac{1}{\rho_{i+1}}
\end{aligned}\tag{25}$$

where $i=1,2,3$ and the superscript or subscript '4' should be replaced by '1'. Note that $p_i^j=p_i^j(\mathbf{x})$, $q_i=q_i(\mathbf{x})$, $\eta=\eta(\mathbf{x})$, $\rho_i=\rho_i(\mathbf{x})$, $d_i=d_i(\mathbf{x})$. This dependence of $p_i^j,q_i,\eta,\rho_i,d_i$ on $\mathbf{x}$ is omitted here and in the sequel for brevity. In addition, let

$$\theta_0(\mathbf{x})=\begin{cases}0 & \text{if } \underset{\sim}{\mathbf{x}}\in P_{E_q}\setminus\overline{E_q}\\ \pi & \text{if } \underset{\sim}{\mathbf{x}}\in L_q\setminus\{\mathbf{y}^1,\mathbf{y}^2,\mathbf{y}^3\}\\ 2\pi & \text{if } \underset{\sim}{\mathbf{x}}\in E_q\\ \theta_i & \text{if } \underset{\sim}{\mathbf{x}}=\mathbf{y}^i,\quad i=1,2,3\end{cases}\tag{26}$$

Finally, introduce the function

$$\theta(\mathbf{x})=\frac{1}{2}\sum_{i=1}^{3}\gamma_i(\mathbf{x})+\operatorname{sign}(\eta)\theta_0(\mathbf{x})\tag{27}$$

On the basis of these definitions, the generic integrals (19) can be expressed as

$$\begin{aligned}
I_1&=\sum_{i=1}^{3}q_i\chi_i(\mathbf{x})-\eta\theta(\mathbf{x})\\
I_1^{\xi}&=\frac{1}{2}\sum_{i=1}^{3}(q_i\tilde{\rho}_i(\mathbf{x})\cos\alpha_i-d_i\chi_i(\mathbf{x})\sin\alpha_i)\\
I_1^{\zeta}&=\frac{1}{2}\sum_{i=1}^{3}(q_i\tilde{\rho}_i(\mathbf{x})\sin\alpha_i+d_i\chi_i(\mathbf{x})\cos\alpha_i)
\end{aligned}\tag{28}$$

and

$$I_3=\frac{1}{\eta}\theta(\mathbf{x}),\quad I_3^{\xi}=\sum_{i=1}^{3}\chi_i(\mathbf{x})\sin\alpha_i,\quad I_3^{\zeta}=-\sum_{i=1}^{3}\chi_i(\mathbf{x})\cos\alpha_i\tag{29}$$

In addition to (29), the generic integrals associated with the double-layer potential (10) read

$$\begin{aligned}
I_3^{\xi\zeta}&=\sum_{i=1}^{3}(q_i\chi_i(\mathbf{x})\cos\alpha_i+\tilde{\rho}_i(\mathbf{x})\sin\alpha_i)\sin\alpha_i\\
I_3^{\xi\xi}&=\sum_{i=1}^{3}(q_i\chi_i(\mathbf{x})\cos\alpha_i+\tilde{\rho}_i(\mathbf{x})\sin\alpha_i)\cos\alpha_i-\eta\theta(\mathbf{x})\\
I_3^{\zeta\zeta}&=\sum_{i=1}^{3}(q_i\chi_i(\mathbf{x})\sin\alpha_i-\tilde{\rho}_i(\mathbf{x})\cos\alpha_i)\sin\alpha_i-\eta\theta(\mathbf{x})
\end{aligned}\tag{30}$$

DOI: 10.1002/nme

Next, the generic integrals for the 'quadruple'-layer potential introduced in (20) can be evaluated as

$$I_5 = \frac{1}{3\eta^2}\sum_{i=1}^{3}\frac{q_i}{d_i}\delta_i(\mathbf{x}) + \frac{1}{3\eta^3}\theta(\mathbf{x}), \quad I_5^{\xi} = \frac{1}{3}\sum_{i=1}^{3}\frac{\delta_i(\mathbf{x})}{d_i}\sin\alpha_i, \quad I_5^{\zeta} = -\frac{1}{3}\sum_{i=1}^{3}\frac{\delta_i(\mathbf{x})}{d_i}\cos\alpha_i \tag{31}$$

and

$$\begin{aligned}
I_5^{\xi\zeta} &= -\frac{1}{3}\sum_{i=1}^{3}\left(\mathscr{L}_i(\mathbf{x})\sin\alpha_i - \frac{q_i}{d_i}\delta_i(\mathbf{x})\cos\alpha_i\right)\sin\alpha_i \\
I_5^{\xi\xi} &= -\frac{1}{3}\sum_{i=1}^{3}\left(\mathscr{L}_i(\mathbf{x})\cos\alpha_i + \frac{q_i}{d_i}\delta_i(\mathbf{x})\sin\alpha_i\right)\sin\alpha_i + \frac{1}{3\eta}\theta(\mathbf{x}) \\
I_5^{\zeta\zeta} &= \frac{1}{3}\sum_{i=1}^{3}\left(\mathscr{L}_i(\mathbf{x})\sin\alpha_i - \frac{q_i}{d_i}\delta_i(\mathbf{x})\cos\alpha_i\right)\cos\alpha_i + \frac{1}{3\eta}\theta(\mathbf{x})
\end{aligned} \tag{32}$$

In the formulae (27) through (32), the sum is performed over the edges L_i $(i=1,2,3)$ of E_q. It is now clear that the format of expressions (27) through (32) is identical for each side L_i of E_q. Also, the singular case, when the source point $\mathbf{x}$ is on the plane of E_q (i.e. $\eta=0$), is simply a special situation that can be effectively dealt with by taking the limit $\eta\to 0$.

3.3. Details of the analytic integration

Formulae (28) through (32) can be summarized into the following result:

Theorem 3.1
In local coordinate systems $\{\mathbf{x}; p_i, q_i, \eta\}$, paralleled to the sides L_i $(i=1,2,3)$ of a flat triangle E_q with origin at a source point $\mathbf{x}\in\mathbb{R}^3$, the generic integrals I_1, I_1^{ξ}, I_1^{ζ}, I_3, I_3^{ξ}, I_3^{ζ}, $I_3^{\xi\xi}$, $I_3^{\xi\zeta}$, $I_3^{\zeta\zeta}$, I_5, I_5^{ξ}, I_5^{ζ}, $I_5^{\xi\xi}$, $I_5^{\xi\zeta}$, $I_5^{\zeta\zeta}$ given in (28) through (32) can be expressed exactly as a sum of analytic formulae over the sides L_i of E_q.

To provide a proof of this theorem, it is important to note that

$$I_3^{\xi\xi} = -\eta^2 I_3 + F_3, \quad I_3^{\zeta\zeta} = -\eta^2 I_3 + J_3 \tag{33}$$

where

$$F_3 = \int_{E_q}\frac{\xi^2+\eta^2}{r^3}\,\mathrm{d}s, \quad J_3 = \int_{E_q}\frac{\zeta^2+\eta^2}{r^3}\,\mathrm{d}s \tag{34}$$

and that

$$I_5^{\xi\xi} = \tfrac{2}{3}I_3 - \eta^2 I_5 + F_5, \quad I_5^{\zeta\zeta} = \tfrac{2}{3}I_3 - \eta^2 I_5 + J_5 \tag{35}$$

where

$$F_5 = \frac{1}{3}\int_{E_q}\frac{\xi^2+\eta^2-2\zeta^2}{r^5}\,\mathrm{d}s, \quad J_5 = \frac{1}{3}\int_{E_q}\frac{\zeta^2+\eta^2-2\xi^2}{r^5}\,\mathrm{d}s \tag{36}$$

With these observations, integrals (19) and (20) can be classified into two groups. In the first group, I_1, I_3 and I_5 can be carried out by careful application of Green's theorem (Stokes' theorem)

DOI: 10.1002/nme

[20–22] resulting in contour integrals over L_q. In the second group that includes I_1^{ξ}, I_1^{ζ}, I_3^{ξ}, I_3^{ζ}, $I_3^{\xi\zeta}$, F_3, J_3, I_5^{ξ}, I_5^{ζ}, $I_5^{\xi\zeta}$, F_5, J_5, exact expressions can first be obtained by straightforward surface integration over E_q and converted to formulae over the edges L_i $(i=1,2,3)$ of the element E_q. In the sequel, an example will be given in each category.

3.3.1. Contour integrals. Consider I_3 as an example in the first group. The treatment of I_1 and I_5 is accomplished in an analogous manner. Recall that P_{E_q} denotes the plane of E_q. Also, recall that $\{\underset{\sim}{\mathbf{x}}; \mathbf{e}_1, \mathbf{e}_2\}$ represents the local orthonormal reference on P_{E_q}, where $\underset{\sim}{\mathbf{x}} \in P_{E_q}$ is the orthogonal projection of the source point $\mathbf{x} \in \mathbb{R}^3$ on P_{E_q} in the direction $\mathbf{e}_3$. In view of (13), one can introduce the position vector $\mathbf{R} \in P_{E_q}$ of an arbitrary field point $\mathbf{y} \in \overline{E_q}$ such that $\mathbf{R} = \mathbf{y} - \underset{\sim}{\mathbf{x}} = \xi \mathbf{e}_1 + \zeta \mathbf{e}_2$ and

$$R = \|\mathbf{y} - \underset{\sim}{\mathbf{x}}\| = \sqrt{\xi^2 + \zeta^2} \tag{37}$$

By virtue of (14) and (37), one can write

$$r = \sqrt{R^2 + \eta^2} \tag{38}$$

For a fixed source point $\mathbf{x}$ and fixed planar triangle E_q, η is a fixed parameter.

Following the idea developed in [14], I_3 can be carried out by first finding a cylindrical symmetric potential $V = V(R; \eta)$ such that

$$\mathrm{div}_s(\nabla_s V) \equiv \frac{1}{R} \frac{\partial}{\partial R} \left(R \frac{\partial V}{\partial R} \right) = \frac{1}{r^3} \tag{39}$$

where the symbols div_s and ∇_s, denote respectively, the surface divergence and the surface gradient on P_{E_q}. It will be clear in the sequel that only the component $\partial V / \partial R$ of $\nabla_s V$ is relevant to the evaluation of I_3. By use of (38) in (39) and integrating once over R, one can write

$$\frac{\partial V}{\partial R} = -\frac{1}{R\sqrt{R^2 + \eta^2}} \tag{40}$$

It is seen from (40) that $\partial V / \partial R$ exhibits a *singular* behavior when $R \to 0$, i.e. when $\underset{\sim}{\mathbf{x}} \to \mathbf{y}$ according to (37). With this observation, it is therefore important to consider two major cases:

(A) *Regular case*: $\underset{\sim}{\mathbf{x}} \in P_{E_q} \backslash \overline{E_q}$. In this case, $\nabla_s V = (\partial V / \partial R)\mathbf{e}_R$ is a continuous and continuously differentiable vector field on $\overline{E_q}$ and one can safely apply Green's theorem for a regular planar surface E_q bounded by a piecewise smooth closed and oriented curve L_q as

$$\int_{E_q} \mathrm{div}_s(\nabla_s V)\, \mathrm{d}s = \int_{L_q} \mathbf{v} \cdot \nabla_s V\, \mathrm{d}l \tag{41}$$

Here $\mathbf{e}_R \in P_{E_q}$ is a unit vector in the radial direction and $\mathbf{v} \in P_{E_q}$ is the unit normal vector to the curve L_q (see Figure 2). Now, the right-hand side of (41) can be carried out in the local coordinate systems $\{\underset{\sim}{\mathbf{x}}; p_i, q_i\}$ associated with each oriented side L_i $(i=1,2,3)$ of E_q. To this end, notice

DOI: 10.1002/nme

that $R^2=(p_i)^2+(q_i)^2$ in $\{\underset{\sim}{\mathbf{x}}; p_i, q_i\}$. By the use of (40) and the fact that $\mathbf{v}\cdot\nabla_s V=(\partial V/\partial R)\partial R/\partial v$ with $\partial R/\partial v=-q_i/R$, one can rewrite (41) as

$$I_3=\int_{L_q}\mathbf{v}\cdot\nabla_s V\,\mathrm{d}l=\sum_{i=1}^{3}\int_{p_i^i}^{p_i^{i+1}}\frac{q_i}{[(p_i)^2+(q_i)^2]\sqrt{(p_i)^2+(q_i)^2+\eta^2}}\,\mathrm{d}p_i \tag{42}$$

In (42), when $i=3$, one should set $p_3^4=p_3^1$. Integration of (42) gives

$$I_3=\frac{1}{2\eta}\sum_{i=1}^{3}\gamma_i(\mathbf{x}) \tag{43}$$

where $\gamma_i(\mathbf{x})$ is expressed in (25).

(B) *Singular case*: $\underset{\sim}{\mathbf{x}}\in\overline{E_q}$. In fact, there are three singular situations to be considered: $\underset{\sim}{\mathbf{x}}$ is located at a vertex $\mathbf{y}^i$ of E_q (i.e. $\underset{\sim}{\mathbf{x}}=\mathbf{y}^i$) as shown in Figure 3(a), $\underset{\sim}{\mathbf{x}}$ is on an edge of E_q (i.e. $\underset{\sim}{\mathbf{x}}\in L_q\backslash\{\mathbf{y}^1,\mathbf{y}^2,\mathbf{y}^3\}$) as illustrated in Figure 3(b), and $\underset{\sim}{\mathbf{x}}$ is an interior point of $\overline{E_q}$ (i.e. $\underset{\sim}{\mathbf{x}}\in E_q$) as depicted in Figure 3(c).

To provide some insights into the foregoing analysis, suppose that the source point $\mathbf{x}$ is situated in $\mathbb{R}^3$ such that $\underset{\sim}{\mathbf{x}}\in\overline{E_q}$ and $\eta=\mathbf{r}\cdot\mathbf{e}_3<0$ (see (13)). With reference to Figure 3(a), assume that $\underset{\sim}{\mathbf{x}}=\mathbf{y}^i$, where $\mathbf{y}^i$ is the ith vertex of E_q. Now, let D_ε denote a disc centered at $\underset{\sim}{\mathbf{x}}$ with radius ε specified as $D_\varepsilon=\{(\xi,\zeta): R=\sqrt{\xi^2+\zeta^2}<\varepsilon\}$, and define $\Omega_\varepsilon=D_\varepsilon\cap E_q$. With such definition, $\partial\Omega_\varepsilon=L_\varepsilon\cup L'_\varepsilon$, where L_ε is the boundary of D_ε lying in $\overline{E_q}$ and L'_ε is the portion of L_q residing in $\overline{D_\varepsilon}$. In $E_q\backslash\overline{\Omega_\varepsilon}$, the vector field $\nabla_s V$ is continuous and continuously differentiable and one can again apply Green's theorem as

$$I_3=\lim_{\varepsilon\to0}\int_{E_q\backslash\overline{\Omega_\varepsilon}}\frac{1}{r^3}\,\mathrm{d}s=\lim_{\varepsilon\to0}\int_{L_q\backslash L'_\varepsilon}\mathbf{v}\cdot\nabla_s V\,\mathrm{d}l+\lim_{\varepsilon\to0}\int_{L_\varepsilon}\mathbf{v}\cdot\nabla_s V\,\mathrm{d}l \tag{44}$$

In (44), $\lim_{\varepsilon\to0}\int_{L_q\backslash L'_\varepsilon}\mathbf{v}\cdot\nabla_s V\,\mathrm{d}l=\int_{L_q}\mathbf{v}\cdot\nabla_s V\,\mathrm{d}l$. This latter integral corresponds to the regular case and can be handled in a similar fashion as in (A). On the arc L_ε, $\mathbf{v}\cdot\nabla_s V=-\partial V/\partial R$ and $R=\varepsilon$. Thus, the last integral in (44) over L_ε can be accomplished as

$$\lim_{\varepsilon\to0}\int_{L_\varepsilon}\mathbf{v}\cdot\nabla_s V\,\mathrm{d}l=\int_{\theta_i}^{0}\frac{-\varepsilon\,\mathrm{d}\lambda}{\varepsilon\sqrt{\varepsilon^2+\eta^2}}=\frac{\theta_i}{|\eta|} \tag{45}$$

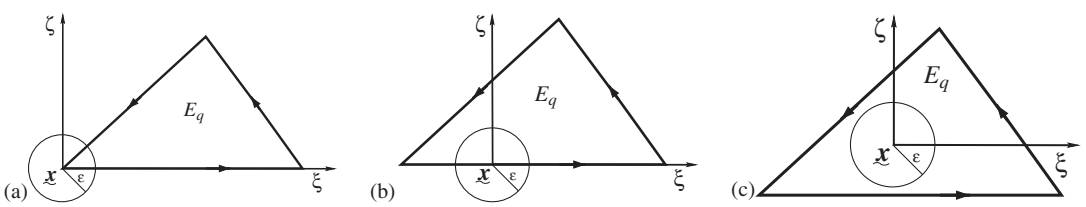

Figure 3. Singular integration over a triangle E_q: (a) vertex case; (b) edge case; and (c) interior case.

DOI: 10.1002/nme

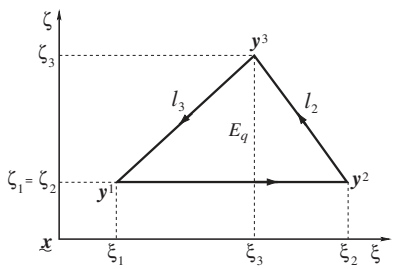

Figure 4. Coordinates in $\{\mathbf{x}; \mathbf{e}_{p_1}, \mathbf{e}_{q_1}, \mathbf{e}_3\} \equiv \{\mathbf{x}; \mathbf{e}_1, \mathbf{e}_2, \mathbf{e}_3\}$ for brute force integration over E_q.

where θ_i is the inclusion angle at the vertex $\underset{\sim}{\mathbf{x}} = \mathbf{y}^i$. With these observations and the assumption that $\eta < 0$, one can rewrite (44) as

$$I_3 = \frac{1}{2\eta} \sum_{i=1}^{3} \gamma_i(\mathbf{x}) - \frac{1}{\eta}\theta_i \tag{46}$$

In the case when $\eta > 0$, it can be shown that $I_3 = (1/2\eta)\sum_{i=1}^{3} \gamma_i(\mathbf{x}) + (1/\eta)\theta_i$. Finally, the edge case (Figure 3(b)) and interior case (Figure 3(c)) can be dealt with in an analogous manner.

3.3.2. Direct surface integration to contour formulae. Consider I_5^{ξ} as an example in the second group of surface integrals. To facilitate the analysis, it is first necessary to permute the vertices of E_q so that L_1 is the longest side. With reference to Figure 4, the equation of the line l_i containing the side L_i $(i = 2, 3)$ can be given as

$$l_i : \xi = K_i^* \zeta + Q_i^*, \quad i = 2, 3 \tag{47}$$

where the slopes K_i^* take the form

$$K_2^* = \frac{\xi_3 - \xi_2}{\zeta_3 - \zeta_2}, \quad K_3^* = \frac{\xi_1 - \xi_3}{\zeta_1 - \zeta_3} \tag{48}$$

With these settings, a brute force calculation of I_5^{ξ} as a double integral can be written as

$$I_5^{\xi} = \tfrac{1}{3}[I(\zeta_3, K_3^*, Q_3^*) - I(\zeta_3, K_2^*, Q_2^*)] - \tfrac{1}{3}[I(\zeta_1, K_3^*, Q_3^*) - I(\zeta_2, K_2^*, Q_2^*)] \tag{49}$$

where the identity $\zeta_1 = \zeta_2$ has been employed and

$$I(\zeta, K, Q) = \frac{\zeta(1 + K^2) + KQ}{(\eta^2(1 + K^2) + Q^2)\sqrt{(K\zeta + Q)^2 + \zeta^2 + \eta^2}} \tag{50}$$

Since $\mathbf{y}^2, \mathbf{y}^3 \in l_2$ and $\mathbf{y}^3, \mathbf{y}^1 \in l_3$, one can use (47) and write

$$\xi_j = K_i^* \zeta_j + Q_i^*, \quad i = 2, 3, \quad j = i, i + 1 \tag{51}$$

DOI: 10.1002/nme

where $\xi_4 \equiv \xi_1$ and $\zeta_4 \equiv \zeta_1$. It is now clear from (51) that the distance from the source point $\mathbf{x}$ to a vertex $\mathbf{y}^j$ of E_q is expressible as $\rho_j = \sqrt{(K_i^* \zeta_j + Q_i^*)^2 + \zeta_j^2 + \eta^2}$ (see (23) when $i=1$). This latter observation together with (50) can be used to rewrite (49) as

$$I_5^{\xi} = \frac{1}{3}\left[\frac{\zeta_2 + \dfrac{K_2^* Q_2^*}{1+(K_2^*)^2}}{\eta^2 + \dfrac{(Q_2^*)^2}{1+(K_2^*)^2}}\frac{1}{\rho_2} - \frac{\zeta_3 + \dfrac{K_2^* Q_2^*}{1+(K_2^*)^2}}{\eta^2 + \dfrac{(Q_2^*)^2}{1+(K_2^*)^2}}\frac{1}{\rho_3}\right] + \frac{1}{3}\left[\frac{\zeta_3 + \dfrac{K_3^* Q_3^*}{1+(K_3^*)^2}}{\eta^2 + \dfrac{(Q_3^*)^2}{1+(K_3^*)^2}}\frac{1}{\rho_3} - \frac{\zeta_1 + \dfrac{K_3^* Q_3^*}{1+(K_3^*)^2}}{\eta^2 + \dfrac{(Q_3^*)^2}{1+(K_3^*)^2}}\frac{1}{\rho_1}\right] \tag{52}$$

One can again employ (51) to reveal that

$$\zeta_j + \frac{K_i^* Q_i^*}{1+(K_i^*)^2} = p_i^j \sin\alpha_i, \quad \frac{(Q_i^*)^2}{1+(K_i^*)^2} = (q_i^j)^2, \quad i=2,3, \quad j=i, i+1 \tag{53}$$

where

$$\begin{aligned} p_i^j &= \xi_j \cos\alpha_i + \zeta_j \sin\alpha_i \\ q_i^j &= -\xi_j \sin\alpha_i + \zeta_j \cos\alpha_i \end{aligned} \tag{54}$$

and

$$\sin\alpha_i = \frac{1}{\sqrt{1+(K_i^*)^2}}, \quad \cos\alpha_i = \frac{K_i^*}{\sqrt{1+(K_i^*)^2}}, \quad i=2,3 \tag{55}$$

Again, in (53) and (54), when $i=3$, $p_3^4 \equiv p_3^1$, $q_3^4 \equiv q_3^1$, also $\xi_4 \equiv \xi_1$, $\zeta_4 \equiv \zeta_1$. Note that formulae (54) and (55) can be extended to side L_1 by taking the limit $K_1^* \to +\infty$ in (55). In what follows, one can now use (53) in (52) to complete the derivation of I_5^{ξ} in terms of exact expressions evaluated along the sides L_i $(i=1,2,3)$ of E_q.

4. RESULTS

To present some numerical results, the limit to the polygonal boundary Γ can now be taken according to (6) via the generic integrals (28) and (29). To this end, special attention should be paid when taking the limit $(\eta \to 0)$ to the plane of a boundary element E_q. As expressed in (29), I_3 is singular as $\eta \to 0$. However, formula (18) reveals that only ηI_3, which is not singular, is indeed relevant to the BIE calculation. In addition, it is important to note that $\theta(\mathbf{x})$ expressed in (27) has a regular discontinuity of the first kind along E_q, i.e. as the source point $\mathbf{x}$ approaches the surface

DOI: 10.1002/nme

E_q from above ($0>\eta\to 0$) or from below ($0<\eta\to 0$), $\theta(\mathbf{x})$ suffers a finite discontinuity on the surface. For this reason, it is convenient to re-define $\theta(\mathbf{x})$ as

$$\theta(\mathbf{x})=\begin{cases}\dfrac{1}{2}\displaystyle\sum_{i=1}^{3}\gamma_i(\mathbf{x})+\theta_0(\mathbf{x}) & \text{if } \eta>0\\[2ex] \dfrac{1}{2}\displaystyle\sum_{i=1}^{3}\gamma_i(\mathbf{x})-\theta_0(\mathbf{x}) & \text{if } \eta\leqslant 0\end{cases} \tag{56}$$

when evaluating the fluxes and potentials on the boundary Γ, and

$$\theta(\mathbf{x})=\begin{cases}\dfrac{1}{2}\displaystyle\sum_{i=1}^{3}\gamma_i(\mathbf{x})+\theta_0(\mathbf{x}) & \text{if } \eta\geqslant 0\\[2ex] \dfrac{1}{2}\displaystyle\sum_{i=1}^{3}\gamma_i(\mathbf{x})-\theta_0(\mathbf{x}) & \text{if } \eta<0\end{cases} \tag{57}$$

when computing the potential u at interior point of the domain Ω. With this observation, analytic expressions (28) and (29) together with (56) can be employed via (6) and (18) to compute the left-hand and right-hand sides of the discretized BIE (7). In particular, it can be shown that the contribution H_{ij}^q to $H_{ij}=\sum_{q=1}^{N_{E_j}} H_{ij}^q$ given by (6), in the singular case when the collocation (source) point $\mathbf{x}^i$ is exactly at a vertex $\mathbf{y}^i$ of E_q, admits the representation

$$H_{ij}^q=\frac{\theta_i}{4\pi}\delta_{ij} \quad \text{(no sum on } i\text{)} \tag{58}$$

In (58), i, j are global indices; δ_{ij} is the Kronecker delta, and θ_i is the inclusion angle at the vertex $\mathbf{y}^i$ of E_q. Indeed, (58) can be derived by use of the double-layer potential $H_j^q(\mathbf{x})$ expressed in (18) and the fact that $\lim_{\eta\to 0}\gamma_i(\mathbf{x})=0$ $(i=1,2,3)$.

To illustrate the utilization of (28) and (29) in the numerical treatment of a boundary-value problem associated with (1), two interior Dirichlet and a mixed problem based on a known oscillatory potential $u(x_1,x_2,x_3)=e^{x_1}\sin x_3+e^{x_3}\cos x_2$ are solved via a collocation BEM. On the surface Γ of the domain of interest Ω, the sought boundary flux is calculated as $t=\mathbf{n}\cdot\nabla u$, where $\nabla u=(e^{x_1}\sin x_3, -e^{x_3}\sin x_2, e^{x_1}\cos x_3+e^{x_3}\cos x_2)$ and $\mathbf{n}$ is the unit outward normal on Γ. This analytic flux is compared against a computed one so that the accuracy of the Dirichlet problem is characterized by L_2-error$=\|\mathbf{t}-\mathbf{t}_e\|/\|\mathbf{t}_e\|$, where $\mathbf{t}$ is the approximated flux at all collocation nodes on Γ, and $\mathbf{t}_e$ is a vector whose components represent the exact flux evaluated at all collocation points on Γ; $\|\cdot\|$ is the usual Euclidean vector norm. In the case of a mixed boundary-value problem, the accuracy is given by L_2-error$=\frac{1}{2}(\|\mathbf{t}-\mathbf{t}_e\|/\|\mathbf{t}_e\|+\|\mathbf{u}-\mathbf{u}_e\|/\|\mathbf{u}_e\|)$. Here $\mathbf{u}_e$ and $\mathbf{u}$ are the exact and computed potentials at all collocation points on Γ. With the L_2-error estimates E_1 and E_2 between two consecutive discretizations of Γ, one can also compute an approximate rate of convergence of the foregoing methodology as

$$\beta=2\frac{\ln(E_2/E_1)}{\ln(N_1/N_2)} \tag{59}$$

where N_1 and N_2 are the respective number of unknowns (collocation points) on Γ. In this study, the linear system (7) is solved iteratively via the BiCGSTAB [23] without preconditioner. Results

DOI: 10.1002/nme

Table I. Top: interior Dirichlet problem on a toroidal domain using piecewise linear shape functions. Bottom: interior Dirichlet problem on an L-shaped domain employing piecewise constant approximations (time in seconds).

N_{col}	Time	L_2-error	β
Torus			
630	0.54	2.327×10^{-1}	—
1292	2.28	1.556×10^{-1}	1.121
2888	11.18	9.889×10^{-2}	1.127
5092	35.68	7.407×10^{-2}	1.019
7432	75.45	5.671×10^{-2}	1.413
11 764	192.20	4.472×10^{-2}	1.034
15 518	336.70	3.821×10^{-2}	1.136
L-shaped domain			
578	0.22	1.413×10^{-1}	—
1236	1.02	1.011×10^{-1}	0.881
2494	4.32	8.199×10^{-2}	0.597
5642	21.77	6.304×10^{-2}	0.644
7426	40.10	5.586×10^{-2}	0.880
11 242	90.26	4.959×10^{-2}	0.574
16 144	203.60	4.584×10^{-2}	0.435

in this section are computed on a single Intel Xeon(EM64T) processor running at 3.2 GHz with 1 MB L2 cache of a dual CPU workstation with a total of 4 GB DDR2 memory.

4.1. Interior Dirichlet problem on a torus

With reference to Figure 1 (left), consider an interior Dirichlet problem for the Laplace equation in a torus Ω centered at $(0,0,0)$ with major radius $R'=6$ and minor radius $r'=2$ such that $\Omega=\{(x_1,x_2,x_3)\in\mathbb{R}^3:(\sqrt{(x_1)^2+(x_2)^2}-R')^2+(x_3)^2<r'^2\}$. Everywhere on the boundary $\Gamma=\partial\Omega$, the potential u is prescribed as $u|_\Gamma=e^{x_1}\sin x_3+e^{x_3}\cos x_2$.

On employing isoparametric piecewise linear elements to discretize the problem, Table I (top) shows the results of the foregoing interior Dirichlet problem in terms of the total execution time (time in seconds) and accuracy on the boundary flux (L_2-error) for several discretizations. In this example, the number of collocation points $N_{\text{col}}=N$, where N is the total number of boundary nodes. Besides, exact expressions given in (28) and (29) have been utilized in the computation. As can be seen from the table, results by the current approach agree very well with the known solution within the linear approximation framework. Indeed, Table I (top) also shows a linear convergence ($\beta\approx1$) of the current methodology.

4.2. Interior Dirichlet problem on an L-shaped domain

With the analytic formulae (28) and (29), one can easily put together the piecewise constant collocation BEM using only I_1 and ηI_3. Assuming that the potential and flux are constant on each boundary element, consider an approximation of an interior Dirichlet problem for the Laplace equation in an L-shaped domain Ω as shown in Figure 1 (right). In this example, $\Omega=\Omega_1\cup\Omega_2$, where

DOI: 10.1002/nme

Table II. Mixed problem on a standard cube using piecewise constant approximations (time in seconds).

N_{col}	Time	L_2-error	β
Standard cube			
588	0.27	1.242×10^{-2}	—
1200	1.12	9.179×10^{-3}	0.848
2352	4.45	7.051×10^{-3}	0.784
5292	24.40	5.246×10^{-3}	0.729
7500	48.51	4.654×10^{-3}	0.687
11 532	112.81	4.030×10^{-3}	0.669
15 552	204.83	3.653×10^{-3}	0.657

$\Omega_1=\{(x_1,x_2,x_3)\in\mathbb{R}^3:0<x_1,x_2<2,0<x_3<6\}$ and $\Omega_2=\{(x_1,x_2,x_3)\in\mathbb{R}^3:0<x_1,x_3<2,0<x_2<4\}$. Again, everywhere on the boundary $\Gamma=\partial\Omega$, the potential u is prescribed as $u|_\Gamma=e^{x_1}\sin x_3+e^{x_3}\cos x_2$.

The results of this exercise are shown in Table I (bottom) in terms of total execution time (time in seconds) and accuracy on the boundary flux (L_2-error). Here, the barycenter of each triangular element represents a collocation point on Γ. Thus, the number of collocation points $N_{\text{col}}=N_E$, where N_E is the total number of boundary elements on Γ. A good agreement with the analytic flux can again be observed from the table at all mesh refinements. The last column of the table reveals that the rate of convergence of the constant element approximation is less than linear. Indeed, the error on the boundary flux L_2-error$=O(h^\beta)$, where the approximate rate of convergence $\beta<1$ and h is the average mesh size on the boundary Γ.

4.3. Mixed problem on a standard cube

Consider a mixed boundary-value problem for the Laplace equation in the standard cube $\Omega=\{(x_1,x_2,x_3)\in\mathbb{R}^3:0<x_1,x_2,x_3<1\}$. The potential $u|_\Gamma=e^{x_1}\sin x_3+e^{x_3}\cos x_2$ is given on the face $\{x_1=0,\ 0\leqslant x_2,x_3\leqslant1\}$, and the flux $t=\mathbf{n}\cdot\nabla u$ is prescribed on the remaining faces, where $\nabla u=(e^{x_1}\sin x_3,-e^{x_3}\sin x_2,e^{x_1}\cos x_3+e^{x_3}\cos x_2)$. On employing a constant element approximation as in Section 4.2, results of the foregoing mixed problem can be seen in Table II for different discretizations. In the table, N_{col} corresponds to the total number of boundary elements on Γ; the total execution time (time) is expressed in seconds; L_2-error$=\frac{1}{2}(\|\mathbf{t}-\mathbf{t}_e\|/\|\mathbf{t}_e\|+\|\mathbf{u}-\mathbf{u}_e\|/\|\mathbf{u}_e\|)$, where $\|\mathbf{t}-\mathbf{t}_e\|/\|\mathbf{t}_e\|$ and $\|\mathbf{u}-\mathbf{u}_e\|/\|\mathbf{u}_e\|$ are the relative errors on the boundary flux and potential, respectively; β is the approximate rate of convergence of the constant element collocation BEM.

5. CONCLUSIONS

In this article, a new set of analytic expressions have been developed for all potentials, defined over a triangular domain, that are commonly found in the computational treatment of 3D singular and hyper-singular BIEs of potential theory. These new exact formulae, which are derived within the linear approximation framework and valid for an arbitrary source point in space, are represented in a uniform format for each edge of the triangular domain. Compared with existing exact expressions for potentials defined over a flat triangle, the recursive format of the proposed formulae is very

DOI: 10.1002/nme

advantageous. Indeed, their subsequent utilization in the hyper-singular Galerkin method alleviates the difficulties associated with the treatment of inherent singularities. In addition, the use of recursive formulae greatly simplifies the implementation of the boundary element code. Sample problems have shown that the new expressions are accurate and stable.

ACKNOWLEDGEMENTS

The submitted manuscript has been authored by a contractor of the U.S. Government under Contract No. DE-AC05-00OR22725. Accordingly, the U.S. Government retains a non-exclusive, royalty-free license to publish or reproduce the published form of this contribution, or allow others to do so, for U.S. Government purposes.

REFERENCES

1. Banerjee PK. *The Boundary Element Methods in Engineering*. McGraw-Hill: London, 1994.
2. Bonnet M. *Boundary Integral Equation Methods for Solids and Fluids*. Wiley: New York, 1995.
3. Hackbusch W. *Integral Equations*: *Theory and Numerical Treatment*. Birkhäuser: Basel, 1995. ISNM.
4. París F, Canãs J. *Boundary Element Method*: *Fundamentals and Applications*. Oxford University Press: New York, 1997.
5. Lutz AD, Gray LJ. Exact evaluation of singular boundary integrals without CPV. *Communications in Numerical Methods in Engineering* 1993; **9**:909–915.
6. Gray LJ, Glaeser JM, Kaplan T. Direct evaluation of hypersingular Galerkin surface integrals. *SIAM Journal on Scientific Computing* 2004; **25**(5):1534–1556.
7. Guiggiani M, Krishnasamy G, Rudolphi TJ, Rizzo FT. A general algorithm for the numerical solution of hypersingular equations. *Journal of Applied Mechanics* 1992; **59**(9):604–614.
8. Tanaka M, Sladek V, Sladek J. Regularization techniques applied to boundary element methods. *Applied Mechanics Reviews* 1994; **47**(10):457–499.
9. Cruse TA, Aithal R. Non-singular boundary integral equation implementation. *International Journal for Numerical Methods in Engineering* 1993; **36**:237–254.
10. Hayami K, Matsumoto H. A numerical quadrature for nearly singular boundary element integrals. *Engineering Analysis with Boundary Elements* 1994; **13**:143–154.
11. Lachat JC, Watson JO. Effective numerical treatment of boundary integral equations: a formulation for three-dimensional electrostatics. *International Journal for Numerical Methods in Engineering* 1976; **10**:273–289.
12. Johnston BM, Johnston PR, Elliott D. A sinh transformation for evaluating two-dimensional nearly singular boundary element integrals. *International Journal for Numerical Methods in Engineering* 2007; **69**:1460–1479.
13. Okon EE, Harrington RF. The potential integral for a linear distribution over a triangular domain. *International Journal for Numerical Methods in Engineering* 1982; **18**:1821–1828.
14. Medina DE, Liggett JA. Exact integrals for three-dimensional boundary element potential problems. *Communications in Applied Numerical Methods* 1989; **5**:555–561.
15. Aimi A, Diligenti M. Numerical integration in 3D Galerkin BEM solution of HBIEs. *Computational Mechanics* 2002; **28**:233–249.
16. Carini A, Salvadori A. Analytical integrations in 3D BEM: preliminaries. *Computational Mechanics* 2002; **28**: 177–185.
17. Rjasanow S, Steinbach O. *The Fast Solution of Boundary Integral Equations*. Springer: New York, 2007.
18. Kress R. *Linear Integral Equations*. Springer: New York, 1999.
19. Nintcheu Fata S. Fast Galerkin BEM for 3D-potential theory. *Computational Mechanics* 2008; **42**(3):417–429.
20. Brand L. *Vector and Tensor Analysis*. Wiley: New York, 1947.
21. Petryk H, Mróz Z. Time derivatives of integrals and functionals defined on varying volume and surface domains. *Archives of Mechanics* 1986; **38**(5–6):697–724.
22. Rahman M. *Advanced Vector Analysis for Scientists and Engineers*. WIT Press: Southampton, 2007.
23. Sleijpen GLG, Fokkema DR. BiCGSTAB(l) for linear equations involving unsymmetric matrices with complex spectrum. *ETNA* 1993; **1**:11–32.

DOI: 10.1002/nme